ACADEMIA ROMÂNĂ
Revue Roumaine de Chimie
http://web.icf.ro/rrch/

Rev. Roum. Chim.,
2018, *63*(5-6), 505-513

Dedicated to Dr. Maria Zaharescu
on the occasion of her 80th anniversary

COMPARATIVE EVALUATION OF PROPERTIES OF SOME NOVEL MALEATED POLYPROPYLENE-SiO_2 COMPOSITES IN CORRELATION WITH THE MORPHOLOGY OF THE FILLER

Fulga TANASĂ* and Mădălina ZĂNOAGĂ

"Petru Poni" Institute of Macromolecular Chemistry, 41A Grigore Ghica Vodă Alley, 700487 Iaşi, Roumania

Received July 31, 2017

The present study is a critical assessment of thermal and mechanical properties of a series of novel composites obtained using a commercially available maleated polypropylene (PP-*g*-MA) and silica (SiO_2) particles having dimensions ranging from micro- to nanometric scale, aiming at correlating the envisaged properties of composites with the morphology of the filler. The presence of the silica particles in the composite formulations entailed increased thermal stability and improved mechanical characteristics, as expected. Still, the experimental data showed a strong dependency of properties on the size of the silica particles as it was observed that nanoparticles caused enhanced effects as compared to the microparticles.

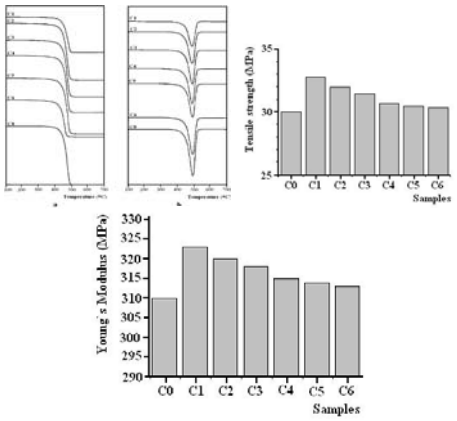

INTRODUCTION

Among the numerous polymers used for composites manufacturing, polypropylene (PP) is one of the most popular thermoplastics due to its attractive combination of properties (low density, high stiffness and toughness, good thermal stability and high heat distortion temperature above 100ºC, chemical resistance and environmental inertness, low moisture uptake, excellent dielectric properties), good processability (readily processable and recycled using the existent technologies), wide range of applications and relatively low production costs.[1,2]

Some of the compatibility issues associated with PP when used in incompatible polymer blends or polymer composites with polarity disparities between components were overcame by different approaches. Thus, grafting acrylic acid (AA) or maleic anhydride (MA) onto PP and the synthesis of silane- or organoborane-modified PP proved to be very good solutions. Such compounds were added to the initial PP-based formulations, as compatibilizing agents, with significantly improved results: reduced difference in the components polarity, increased melt flow rate, lower interfacial tension, modulated crystallinity.[3-5] In the case of the maleated polypropylene (PP-*g*-MA), the compatibilization effects in PP blends and composites were assigned to its chemical structure (presented in Fig. 1) that allowed not only enhanced interactions at the interface, but also contributed to the formation of the interphase or even chemical bonds (when applicable).

* Corresponding author: ftanasa@icmpp.ro

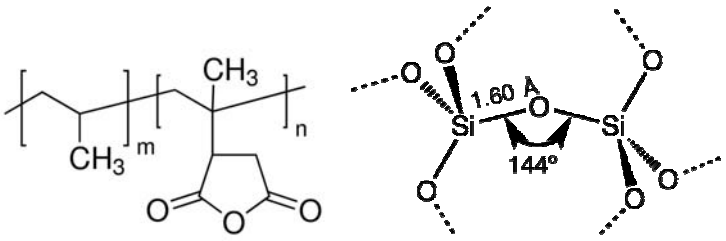

Fig. 1 – Chemical structure of maleated polypropylene (left) and silica (right).

In this regard, structural studies evidenced the presence of grafted poly(maleic anhydride) in PP-*g*-MA and succinic anhydride end groups, as well as pendant,[6-10] although other reports concluded that the homopolymerization of maleic anhydride did not occur in PP-*g*-MA.[11] The phase morphology in PP/PP-*g*-MA-based formulations highly depends on the molecular weight and the content in MA. Thus, when maleated polypropylene has low molecular weight and high MA content, the phase separation occurs, while reversed ratios lead to co-crystallization.[5] These effects may be attributed to thermodynamic factors, as well as to crystallization kinetics, and strongly affect the mechanical properties of the PP-*g*-MA compatibilized PP-based materials.

Composites made of PP and silicon (Si)-containing fillers, either particulate or layered, have been extensively studied as the new materials exhibited remarkable enhancement of properties upon the addition of low amounts of filler. Issues of interest range within large limits: interfacial interactions at the PP-silica particles interface, using both neat[12] and modified particles (fumed silica particles,[13] polymer-grafted silica particles[14] or silica-coated particles[15]), as well as layered silicates,[16] in various compatibilized formulations (using chemically modified clays[17] or compatibilizers such as PP-*g*-MA[18]); effects of the formulation on the characteristics of the composites;[19] correlations between methods of preparation (melt blending,[20] solid state modification,[21] sol-gel process,[22] *in situ* crosslinking,[23] biomimetic silicification[24]) and composites properties.

Under these circumstances and given that numerous reports focused on the effects of the morphology (shape and size) of silica particles on the PP-based composites characteristics, the investigation of direct interactions between PP-*g*-MA and neat SiO_2 particles is of interest, from both theoretic (a better understanding of the compatibilization effect, discrimination of the particular contribution of the PP-*g*-MA/SiO_2 interactions to the overall effect) and practical point of view. The present study is a critical assessment of properties of a series of novel composites obtained using commercially available maleated polypropylene (PP-*g*-MA) and silica (SiO_2) particles with a granulometric distribution ranging from micro- to nanometric scale. In this report, only the size of the particles was discussed, as the working premise was that all particles have the same spherical shape, limiting thus the number of variables influencing the experimental results.

RESULTS AND DISCUSSION

The most addressed problems in compatibilized composites are related to interactions. In particulate composites, particle-polymer interactions are responsible for the micromechanical deformations and macroscopic behaviour, while particle-particle ones lead to secondary agglomeration phenomena.[25] Since the particles employed in our study do not have functionalized surface, the particle-particle interactions are not expected to contribute in a significant ratio, and, therefore, the study will focus on polymer-particle interactions.

Sample codes of the composites evaluated in this study are presented in Table 1.

Table 1

PP-*g*-MA composites with silica particles (3% particles volume fraction)

Sample code	Particle size
C0 (PP-*g*-MA)	-
C1	50 nm
C2	200 nm
C3	400 nm
C4	2 μm
C5	40 μm
C6	100 μm

Composites morphology

The properties of composites, either particulate or fiber reinforced, are strongly dependent on their morphology, which is significantly influenced by the nature, shape and size of the filler, as well as its dispersion, compatibility between composite

components, processing parameters, etc. At nanometric scale, morphology of the filler particles becomes more important as the short range matrix-particle interactions are the driving force in terms of acquising enhanced properties.

In the case of the studied PP-*g*-MA/SiO_2 composites, the SEM micrographs revealed a fair dispersion of silica nanoparticles inside the matrix for the considered samples, as shown in Fig. 2.

Usually, when spherical nanoparticles are used, the composites had an inhomogeneous aspect due to difficulties to evenly distribute the filler inside the matrix. So, an improved dispersion is granted by a wise choise of processing parameters in order to avoid secondary agglomeration of nanoparticles. In the selected PP-*g*-MA/SiO_2 samples, a good dispersion was achieved as a result of using maleate PP as matrix.

As noticed in the micrographs (Fig. 2d), the debonding has occurred during the sample preparation (cryogenically breaking under liquid nitrogen – see Experimental section), evidenced by particles remained out-of-plane and voids left in the polymer bulk after particles were plucked from material, despite the frozen state of samples. This is an illustration of the micromechanical deformation processes that usually take place in particulate polymer composites under the external stress concentration which is causing local deformations.[25] An improved interfacial adhesion is expected to significantly reduce the debonding and this can be achieved by the chemical functionalization of the particles surface. In this way, new chemical bonds are formed between functional groups from particles and polymer matrix, adding to the interface interactions.

Another feature observed from the SEM images is the absence of the cavitation, phenomenon which is a characteristic of PP processed by melt mixing.[26,27] The same behaviour was previously noticed in the case of PP-clay nanocomposites, as well.[28] The cavitation phenomenon depends on the processing parameters (temperature and rate of deformation),[27] but mainly on the amorphous: crystalline ratio, as the amorphous phase grants the break strength, while the crystalline phase is responsible for the initiation of crystals sliding.[26] Thus, it is possible to control the occurrence of the cavitation by tuning this ratio. In our case, the chemical modification of PP, objectified by the branched structure of the PP-*g*-MA, entailed a modified amorphous:crystalline ratio and, hence, an altered behaviour, when no cavitation occurred after melt mixing.

Thermal behaviour of composites

Data obtained by the means of DSC (heating and cooling scans) are presented in Fig. 3 and 4, and Table 2. The DSC study on the melting of the considered composite samples (Fig. 3) revealed the change in the endothermic transition peaks as result of the distinct behaviour of each material.

In the initial and final stages of scanning, all samples showed rather similar behaviour, although a certain grouping of thermograms is evident. Thus, samples containing nanoparticles (C1-C3) can be easily discriminated from those having micrometer sized particles (C4-C6). A slight increase was recorded for the onset temperature of the melting which is explained by the addition of silica particles into the polymer. But in the case of samples C1-C3, it is noticeable that adding the nanosized particles has caused higher onset temperatures. The highest endothermic peaks have been registered for C1 (50nm) and C2 (200nm). In this composites series, the larger the particles, the lower the onset temperature values, and the wider the peaks. This is a good indication that the crystallinity of the composites is different and depends on the size of the particles: the smaller the particles, the higher the crystallinity, as confirmed by other studies.[29,30] At the same time, the broad range of melting intervals of composites containing microparticles suggested that the crystallites have a wide dimensional distribution.

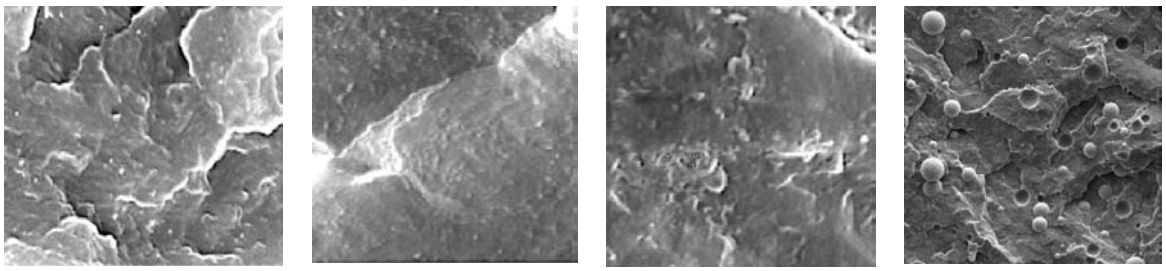

a b c d

Fig. 2 – SEM micrographs: a –C1(50 nm); b – C2 (200 nm); c – C3 (400 nm); d – C4 (2 μm).

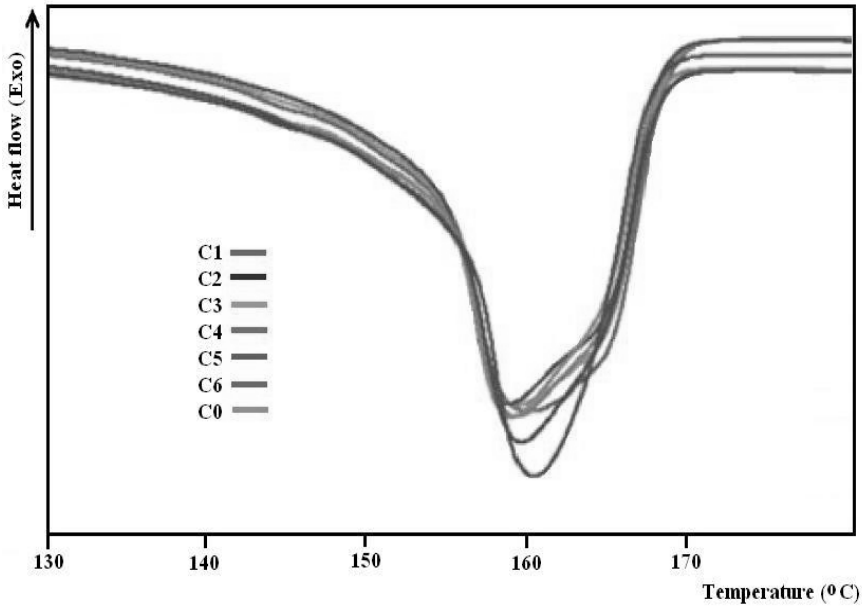

Fig. 3 – DSC scans on heating of the neat PP-*g*-MA (C0) and PP-*g*-MA – silica composites (C1-C6).

Table 2

Thermal data from DSC scans performed on the neat PP-g-MA (C0) and composites C1-C6 during heating and cooling

Sample code	T_m (°C)	ΔH_m (J/g)	T_{exo} (°C)	ΔH_c (J/g)
C0	156.95	63.175	113.91	91.673
C1	160.99	107.899	120.07	109.993
C2	159.85	106.988	118.17	105.730
C3	159.34	104.467	117.86	103.900
C4	158.71	103.973	116.025	102.580
C5	158.27	102.770	115.67	98.990
C6	157.97	100.067	114.31	95.355

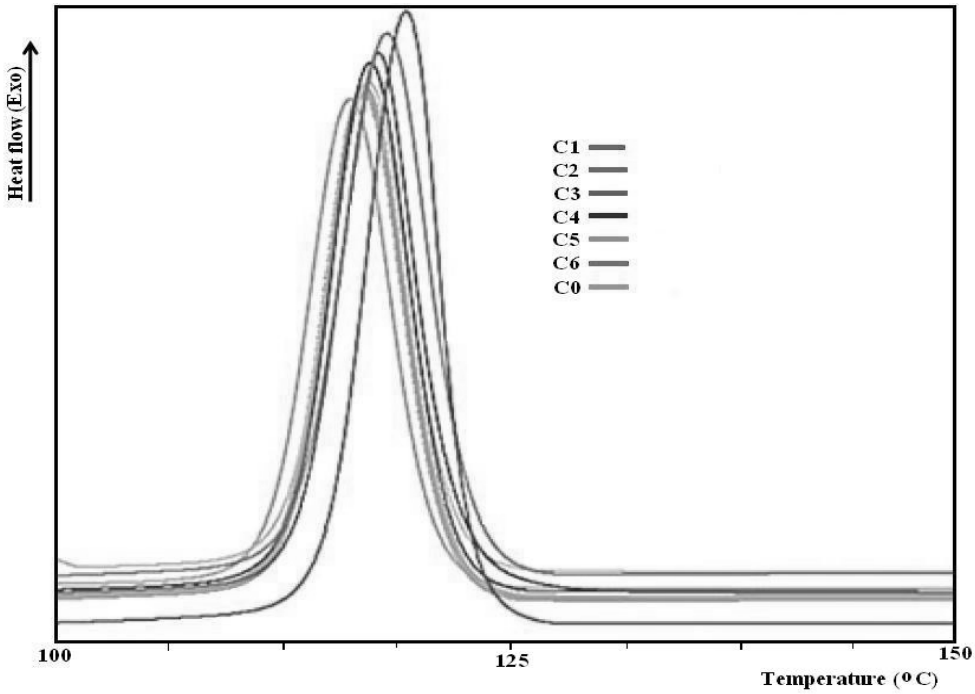

Fig. 4 – DSC scans on cooling of the neat PP-*g*-MA (C0) and PP-*g*-MA – silica composites (C1-C6).

The crystallization behaviour of composites C1-C6 was evaluated by DSC scanning during cooling (Fig. 4).

Comparing the registered data, it was noticed that T_{exo} decreased along with the increasing size of particles. The same trend was observed for ΔH_c, as well. It became evident that the distinct crystallization exotherms are due to the formation of different crystalline structures during cooling. There is an increase in the overall rate of crystallization along with the decreasing size of particles in the composites series, phenomenon that was confirmed by studies on the rate of nucleation.[29,31,32] Thus, the smaller the particles (C1-C3), the higher the rate of nucleation, which led to the formation of large numbers of crystallites of small dimensions. When the cooling rates are lower, a reduced number of crystallites of large dimensions is expected to yield in composites with nanometer sized particles. Control over this specific behaviour might, therefore, prove to be a useful tool in tuning the rheologic properties of these composites.

The thermal stability of composites was evaluated by TGA and data are shown in Fig. 5 and Table 3.

The TG-DTG data showed that the thermal degradation of neat PP-*g*-MA (C0) and PP-*g*-MA – silica composites (C1-C6) starts above 350-360°C, evolves in a single stage and ends at temperatures below 600°C. This behaviour is due to the thermal stability of both components: on the one hand, the maleated PP used in this study has a density comparable with that of high density polyethylene (HDPE) (HDPE density ranges from 0.935 to 0.96 g/cm³, while the PP has a density of 0.934 g/mL at 25°C) and contents a rather low amount of maleic anhydride (8-10%); on the other hand, silica particles are thermally stable. Typically for composites, a high termal stability is usually reached when particles are well dispersed into the matrix (although the aggregation tendency of fillers strongly increases with the decreasing particles size; hence, in nanocomposites the aggregation is practically unavoidable, regardless the preparation protocol[25]), and have a good wettability in relation to the polymer matrix, which stands for a good coverage of particles by the polymer. Thus, this enveloping layer limits the diffusion towards exterior of volatiles produced during the thermal degradation. At the same time, the char formed around particles acts also as a barrier preventing the heat, as well as volatiles, diffusion. Therefore, the smaller the particles, the more intense the interfacial interactions with the matrix. These phenomena were confirmed by the recorded TGA data.

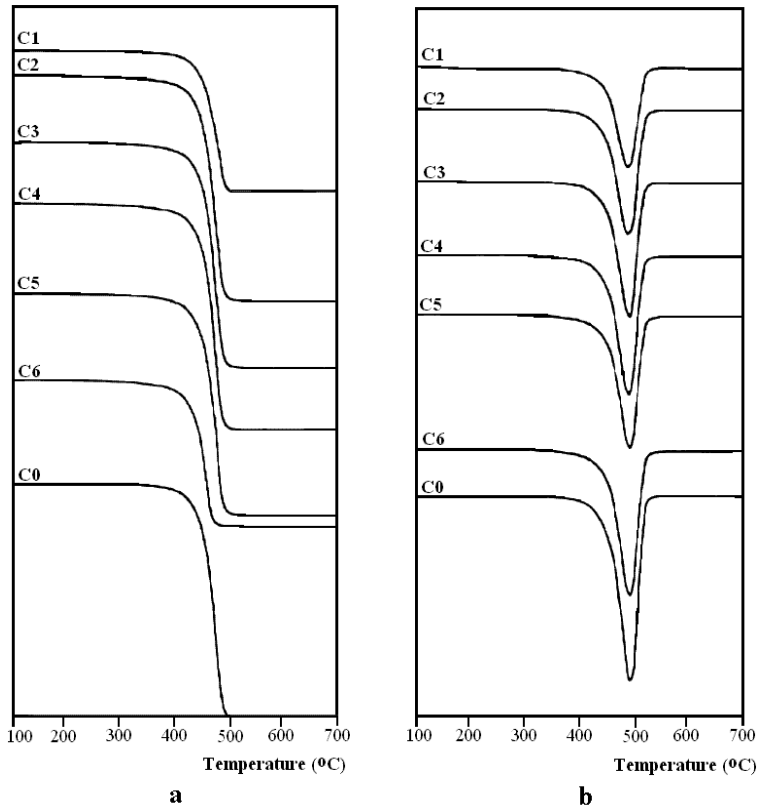

Fig. 5 – Thermal stability of the neat PP-*g*-MA (C0) and PP-*g*-MA – silica composites (C1-C6): a – TG data; b – DTG data.

Table 3

Thermal parameters of the neat PP-*g*-MA (C0) and PP-*g*-MA – silica composites (C1-C6)

Sample code	T_{onset} (°C)	T_{end} (°C)	$T_{inflection}$ (°C)	Char yield (%)
C0	410.00	489.10	440.50	0.279
C1	445.10	486.18	474.00	5.23
C2	444.08	485.94	472.89	4.89
C3	442.90	484.26	471.75	4.57
C4	438.87	483.89	469.35	4.18
C5	433.55	485.05	469.99	3.88
C6	431.75	475.16	443.05	3.56

Comparing the onset temperature values summarized in Table 3, it is easy to notice their decreasing trend along with the increasing particles size, observation valid for the char yield values, as well, which is a clear indication of the enhanced thermal stability of nanocomposites (samples C1-C3).

As for the thermal degradation mechanism, it is within reason to presume that it is dominated by the chain scission reactions (primary and secondary radicals formed by *β*-scissions, tertiary radicals formed *via* rearrangement reactions, volatile alkenes and short polymer chains with a terminal double bond resulted also from *β*-scissions),[33-36] favoured by the presence of pendant oxygen-containing functional groups and by the branched structure of PP-*g*-MA.

Mechanical properties

Mechanical properties of polymer-silica composites and nanocomposites highly depend on various factors, such as: properties of the polymer matrix; silica particles size (spherical shape), loading and distribution; interfacial interactions between filler (raw or functionalized) and matrix (neat, functionalized or in the presence of a compatibilizing agent), etc.

The interfacial adhesion is one key factor significantly related to the mechanical properties of composites, in so far as the strong interfacial interactions entail high tensile strength and low elongation values. The effect of the particles size on the mechanical properties of composites is a result of limitations induced by the inorganic filler on the mobility and deformation of the polymer matrix. This mechanical restraint occurs due to the dynamic balance between the attraction potential among segments of the polymer chain and the repulsive potential of the polymer when it is in the vicinity of the solid particles. The strength of the particle restraint depends on the properties of the filler and matrix.[37]

These interactions also depend on the area of the contacting surfaces (specific surface area of the filler): smaller particles have larger surface area and that leads to an increased yield stress. Another important structural factor must be considered, as well: small particles tend to form primary (resulted from particles production, prior to composites processing) and secondary aggregates (formed during composites processing by melt mixing), tendency that negatively influences mechanical properties (as the stress-strain dependency in nanocomposites significantly exceeds classical micromechanics predictions); for particles having specific surface area over $5m^2/g$, the aggregation tendency becomes significant.[38,39]

Data recorded from mechanical tests are summarized in Table 4 and graphically illustrated in Fig. 6.

Table 4

Mechanical properties of the neat PP-*g*-MA (C0) and PP-*g*-MA – silica composites (C1-C6)

Sample code	Tensile strength (MPa)	Young`s modulus (MPa)
C0	30.00	310
C1	32.80	324
C2	31.98	320
C3	31.41	319
C4	30.67	315
C5	30.43	314
C6	30.35	313

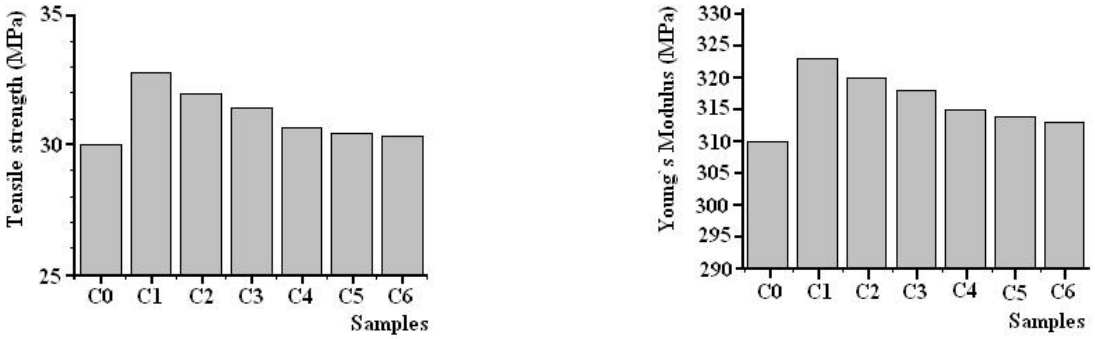

Fig. 6 – Tensile strength (A) and Young`s modulus (B) of the neat PP-*g*-MA (C0) and PP-*g*-MA – silica composites (C1-C6).

The tensile strength in particulate nanocomposites illustrates the stress transfer between the filler and matrix, significant reinforcing effects being observed when strong interfacial interactions take place over extended interface areas. The thicker the polymer layer around particles, the better the stress transfer. On the other hand, if the filler content exceeds a certain value, a rigid skeleton is formed, made of neighboring particles insufficiently covered by polymer, yielding in brittle composites with increased rigidity. Taking the tensile strength value for the neat PP-*g*-MA (30 MPa) as reference, the most intense reinforcing effect was recorded for sample C1 (the one containing the smallest particles), though samples C2 and C3 had comparable, yet slightly lower, strength values (as presented in Table 4 and Fig. 6).

This behaviour can be attributed to the hydrogen bonds that occurred between H atoms of the polymer (PP-g-MA) and O atoms bearing available electrons not involved in covalent bondings in silica particles, which yielded in improved interfacial adhesion and, subsequently, higher tensile strength.

The same tendency can be easily noticed in the case of the Young`s modulus, confirming that the elastic modulus in particulate nanocomposites is generally determined by the elastic properties of polymer matrix, filler loading and particles aspect ratio.[40] It is well known that elastic modulus is a stiffness parameter which governs by the size of particles and their amount. Since the inorganic particles are rigid and have a much higher stiffness than the thermoplastic matrix considered, the composite elastic modulus can be readily improved by adding either micro- or nanoparticles, as confirmed by literature data.[29,41-43]

The effect decreased along with the increasing size of particles, so that the values of the Young`s modulus for samples C5 and C6 (containing particles of 40 and 100μm) are slightly different from that of the neat PP-*g*-MA.

The elastic behaviour of these PP-*g*-MA - silica composites is well described by the theoretic model already reported in the literature,[41,44] that correlates the interfacial adhesion and the fracture mechanism in nanocomposites filled with spherical particles, and takes into consideration the voids formation and their evolution under stress (Fig. 7).

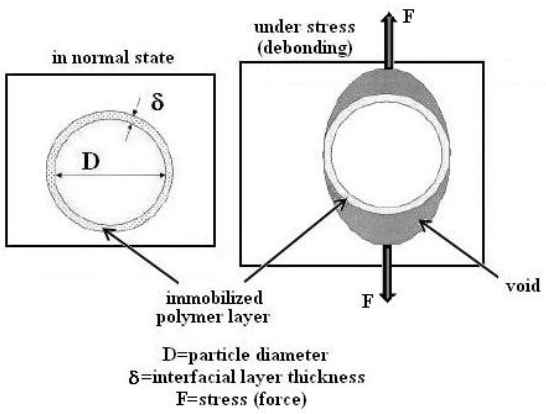

Fig. 7 – The theoretic model that correlates the interfacial adhesion and the voids formation under stress in nanocomposites filled with spherical particles (adapted after ref. 44).

Generally, toughening in rigid filler-containing composites occurs when particles detach from the matrix, creating voids around them and allowing the interparticle ligaments to deform plastically under stress.[45] It has been proven that spherical particles can facilitate the development of microvoids and activate the dilatational yielding in the distorted zone in the vicinity of the fracture surface.[44] The voids act towards the reduction of the macroscopic plastic resistance of the material, and, thereby, can potentially increase the fracture strain and the overall toughness. Ideally, the voids are not likely to appear immediately upon the application of stress, as this may reduce the Young`s modulus.

EXPERIMENTAL

Materials and processing

Silica particles of various size ranging from nano- to micrometer scale, namely 50, 200, 400nm and 2μm (NanoCym, Scottsdale, AZ, USA) and 40 and 100μm (Supelco®, Sigma-Aldrich Chemie GmbH, Taufkirchen, Germany), were used after drying (24 h in a vacuum oven at 70°C and 50 mmHg vacuum). In order to limit the number of variables to be taken into consideration, the particles were considered to have a perfect spherical shape and the filler amount was constant (3% as particles volume fraction) in all formulations.

The matrix of composites was a commercially available PP-*g*-MA (Sigma-Aldrich Chemie GmbH, Taufkirchen, Germany) and it was used after a drying stage (8 h in a vacuum oven at 70°C and 50 mmHg vacuum) in order to remove moisture before mixing with silica particles and further melt blending. Properties: average molecular weight 9100, density 0.934 g/mL at 25°C, maleic anhydride content 8-10%, viscosity 0.4 Pa·s, melting temperature 156°C.

Composites were obtained as follows: after drying, the pre-calculated amounts of silica particles and polymer were premixed in a tumble mixer, then fed to a Haake Rheocord 9000 mixer. The processing parameters were set as to enable a good dispersion of particles within the matrix: temperature=190°C, rotating speed=100 rpm; mixing time = 7 min.

Characterization

The morphological study employed the scanning electron microscopy (SEM) and it was run using a VEGA II SBH scanning electron microscope manufactured by TESCAN (Brno, Czech Republic). Samples were cryogenically fractured after immersion in liquid nitrogen for 30-50 min, then gold coated for an enhanced contrast of phases. The examination under the electron beam was performed using an operating voltage of 30kV.

The thermal behaviour of composites was assessed by both differential scanning calorimetry (DSC) and thermo-gravimetric analysis (TGA). DSC measurements were run under nitrogen atmosphere by using a TA instrument from Perkin-Elmer (USA), Pyris Diamond model, at a heating rate of 10°C/min under dry N_2 atmosphere. The specimens were heated up to 200°C. The melting temperature (T_m) and enthalpy (ΔH_m), and crystallization temperature (T_{exo}) and enthalpy (ΔH_c) were calculated after the melt-crystallization process. The TGA was performed on a Mettler Toledo TGA-SDTA 851 device, in air stream, with a heating speed of 10 K/min, in the temperature range of 25-700°C, using samples of 4-6 mg. During testing, the heating unit was flushed under a continuous air flow of 30 mL/min.

The mechanical properties of composites (tensile strength and modulus) were determined according to ASTM D 638–01 (tensile properties) and ASTM D790–00 (flexural properties) specifications. A mechanical tensile machine (FU-1000; Rauenstein, Germany) was employed; the crosshead speed was set at 20 mm/min and the dimensions of samples were 150x10x5 mm. All samples were conditioned at a temperature of 23±2°C and relative humidity (RH) of 50±5%, for at least 40 h prior to testing. At least five samples were tested for each measurement.

CONCLUSION

This study is a critical assessment of thermal and mechanical properties of a series of novel composites made of commercially available maleated polypropylene (PP-*g*-MA) and silica (SiO_2) particles having dimensions ranging from micro- to nanometric scale. The experimental results confirmed the strong dependency of properties on the size of the silica particles, namely the nanoparticles caused enhanced effects as compared to microparticles.

The thermal stability of composites increased by incorporation of silica spheres, as compared to the neat polymer, and the increment increased along with the decreasing size of particles. The melting temperatures indicated that the larger the particles, the lower the onset temperature values, and the wider the peaks. As for the crystallization dynamics, it was confirmed that the smaller the particles, the higher the crystallinity. At the same time, the broad range of melting intervals of composites containing microparticles suggested that the crystallites have a wide dimensional distribution. It can be concluded that controlling the crystallization rate, the number and size of crystallites, respectivelly, it might be possible to tune the rheologic properties of these materials.

Experimental results proved that the addition of silica particles strongly affected the stress-strain dependence. Thus, it was found that Young's modulus and tensile strength increased along with the decreasing size of particles. These data implied that the smaller particles lead to the formation of more crystallites of small dimensions able to contribute to the stress transfer throughout the matrix, yielding in composites with enhanced strength at break.

Therefore, the use of particles of different size might improve the load transfer in certain composites, as they play complementary roles: smaller particles are involved in the stress transfer, while the medium size particles dissipate the larger ones that are stress concentrators and, consequently, act as crack initiators. On the other hand, considering the type and intensity of interfacial interactions that occurred between PP-*g*-MA and silica particles, even more intense intractions are expected when functionalized silica particles of different size are employed in the same formulation. These assertions can be useful starting hypotheses for further studies.

REFERENCES

1. X.-Y. Ye and Z.-K. Xu, "Polypropylene fabrics", in: "Polypropylene Synthesis, Application and Environmental Concerns", L. P. Silva and E. F. Barbosa (Eds.), Nova Science Publishers, New York, 2013, p. 11-37.
2. M. M. Francis Jr., "Polypropylene and thermoplastic olefins nanocomposites", in "Dekker Encyclopedia of Nanoscience and Nanotechnology", C. I. Contescu and K. Putyera (Eds.), Second Edition, Vol. V, CRC Press, 2008, p. 3509-3524.
3. W. J. Kissel, J. H. Han and J. A. Meyer, "Polypropylene: Structure, Properties, Manufacturing Processes, and Applications", in "Handbook of polypropylene and polypropylene composites", H. G. Karian (Ed.), 2nd edition, Marcel Decker, Inc., New York, 2003, p. 15-37.
4. D. Roberts and R.C. Constable, "Chemical Coupling Agents for Filled and Grafted Polypropylene Composites", in "Handbook of polypropylene and polypropylene composites", H. G. Karian, (Ed.), 2nd edition, Marcel Decker, Inc., New York, 2003, p. 28-68.
5. K. Cho, F. Li and J. Choi, *Polymer,* **1999,** *40*, 1719-1729.
6. B. De Roover, M. Sclavons, V. Carlier, J. Devaux, R. Legras and A. Momtaz, *J. Polym. Sci. Part A Polym. Chem.,* **1995,** *33*, 829-842.
7. B. De Roover, J. Devaux and R. Legras, *J. Polym. Sci. Part A: Polym. Chem.,* **1996,** *34*, 1195-1202.
8. G. E. Myers, I. S. Chahyadi, C. A. Coberly and D. S. Ermer, *Int. J. Polym. Mater.*, **1991,** *15*, 21-44.
9. G. de Vito, N. Lanzetta, G. Maglio, M. Malinconico, P. Musto and R. Palumbo, *J. Polym. Sci. Polym. Chem. Ed.,* **1984,** *22*, 1335-1347.
10. K. E. Russell and E. C. Kelusy, *J. Polym. Sci. Part A: Polym. Chem.,* **1988**, 26, 2273-2280.
11. W. Heinen, M. van Duin, C. H. Rosenmoller, C. B. Wenzel, H. J. M. de Groot and J. Lugtenburg, *Macromolecules,* **1996**, *29*, 1151-1157.
12. M. F. Omar, M. A. Hazizan and A. A. Zainal, *Mater. Des.,* **2013**, 45, 539-547.
13. D. N. Bikiaris, G. Z. Papageorgiou, E. Pavlidou, N. Vouroutzis, P. Palatzoglou and G. P. Karayannidis, *J. Appl. Polym. Sci.*, **2006**, 100, 2684-2696.
14. M. Z. Rong, M. Q. Zhang, S. L. Pan and K. Friedrich, *J. Appl. Polym. Sci.*, **2004,** *92*, 1771-1781.
15. M. Rinastiti, M Ozcan, W. Siswomihardjo and H. J. Busscher, *Journal of Dentistry,* **2010**, *38*, 29-38.
16. J. P. G. Villaluenga, M. Khayet, M. A. Lopez-Manchado, J. L. Valentin, B. Seoane and J. I. Mengual, *Eur. Polym. J.,* **2007**, *43*, 1132-1143.
17. J. W. Gilman, C. L. Jackson, A. B. Morgan and R. Harris, Jr., *Chem. Mater.*, **2000**, *12*, 1866-1873.
18. C. M. Koo, M. J. Kim, M. H. Choi, S. O. Kim and I. J. Chung, *J. Appl. Polym. Sci.*, **2003***, 88*, 1526-1535.
19. S. S. Hwang and P. P. Hsu, *JIEC*, **2013**, *19*, 1377-1383.
20. D. Pedrazzoli and A. Pegoretti, *Compos. Sci. Technol.,* **2013**, *76,* 77-83.
21. S. Jain, H. Goossens, F. Picchioni, P. Magusin, B. Mezari and M. van Duin, *Polymer,* **2005**, *46*, 6666-6681.
22. D. Sun, R. Zhang, Z. Liu, Y. Huang, Y. Wang, J. He, B. Han and G. Yang, *Macromolecules,* **2005**, *38,* 5617-5624.
23. H. Z. Tong, H. R. Wen, L. M. Yu, Z. R. Min and Q. Z. Ming, *Compos. Sci. Technol.,* **2008,** *68*, 2858-2863.
24. H. C. Yang, J. K. Pi, K. J. Liao, H. Huang, Q. Y. Wu, X. J. Huang and Z. K. Xu, *ACS Appl. Mater. Interfaces*, **2014**, *6*, 12566-12572.
25. B. Pukanszky, *Eur. Polym. J.*, **2005**, *41*, 645-662.
26. A. Pawlak and A. Galeski, *J. Polym. Sci., Part B: Polym. Phys.*, **2010**, *48*, 1271-1280.
27. A. Pawlak and A. Galeski, *Polymer*, **2010**, *51*, 5771-5779.
28. M. Zanoaga and F. Tanasa, *Rev. Roum. Chim.*, **2016**, *61*, 373-380.
29. M. H. Alaei, P. Mahajan, M. Brieu, D. Kondo, S. J. A. Rizvi, S. Kumar and N. Bhatnagar, *Iran. Polym. J.*, **2013,** 22, 853-863.
30. S. H. Kim, S. H. Ahna and T. Hirai, *Polymer*, **2003**, *44*, 5625-5634.
31. S. Jain, H. Goossens, M. van Duin and P. Lemstra, *Polymer*, **2005**, *46*, 8805-8818.
32. M. Modesti, A. Lorenzetti, D. Bon and S. Besco, *Polym. Degrad. Stab.*, **2006**, *91*, 672-680
33. H. Bockhorn, A. Hornung, U. Hornung and D. Schawaller, *J. Anal. Appl. Pyrolysis*, **1999**, *48*, 93-109.
34. R. P. Lattimer, *J. Anal. Appl. Pyrolysis*, **1993**, *26*, 65-92.
35. E. Kiran and J. K. Gillham, *J. Appl. Polym. Sci.*, **1976**, *20*, 2045-2068.
36. K. Pielichowski and J. Njuguna, "Thermal Degradation of Polymeric Materials", Smithers Rapra Publishing, Shawbury, United Kingdom, 2005.
37. A. D. Drozdov and A. Dorfmann, *Comput. Mater. Sci.*, **2001**, *21*, 395-417.
38. A. Dorigato, Y. Dzenis and A. Pegoretti, *Mech. Mater.*, **2013**, *61*, 79-90.
39. A. Lazzeri, Y. S. Thio and R. E. Cohen, *J. Appl. Polym. Sci.*, **2004**, *91*, 925-935.
40. S. Y. Fu, X. Q. Feng, B. Lauke and Y. W. Mai, *Composites: Part B*, **2008**, *39*, 933-961.
41. F. Tanasă, M. Zănoagă and R. Darie, *Proceedings of the International Conference AFASES,* **2014**, 241-249 (available on-line at http://www.afahc.ro/ro/afases/2014/mecanica/Tanasa_Zanoaga_Darie.pdf).
42. J. Cho, M. S. Joshi and C. T. Sun, *Compos. Sci. Technol.*, **2006**, *66*, 1941-1952.
43. J. Gao, J. Li, B. C. Benicewicz, S. Zhao, H. Hillborg and L. S. Schadler, *Polymers*, **2012**, *4*, 187-210.
44. A. Lazzeri and C. B. Bucknall, *Polymer*, **1995**, *36*, 2895-2902.
45. B. Pukanszky, "Particulate filled polypropylene composites", in "Polypropylene: An A-Z Reference", J. Karger-Kocsis (Ed.), Kluwer Publishers, Dordrecht, 1999, p. 574-580.